(M.A.) from the Ministry of Education, Culture, Sports, Science and Technology of Japan.

Sir, Generalized pustular psoriasis (GPP) is a rare but severe form of psoriasis that is sometimes life threatening. It is characterized by sudden, repeated episodes of high-grade fever, generalized rash and disseminated pustules. The pathogenesis is unclear except for familial GPP, whose cause was recently identified as homozygous or compound heterozygous mutations in the *IL36RN* gene, also known as *IL1F5*, encoding the interleukin 36 receptor antagonist (IL36RN)[1, 2].

IL36RN is primarily expressed in the skin[3], and is an antagonist of three cytokines that belong to the interleukin-1 family: interleukin-36α, interleukin-36β, and interleukin-36γ, which are also known as interleukin-1F6, interleukin-1F8 and interleukin-1F9, respectively[4, 5]. These cytokines activate several proinflammatory signaling pathways, such as the nuclear factor-κB and mitogen-activated protein kinase pathways[6, 7].

We have followed a Japanese male patient with GPP, and *IL36RN* mutation analysis revealed the previously unreported homozygote nonsense mutation p.Arg10X.

A 68-year-old man presented with recurrent episodes of localized sterile pustules with erythema but without scaly erythematous plaques, on the extremities (Figure 1a, b) and the trunk, but not on the palmoplantar areas. He had been suffering from similar eruptions since the age of 34. He

once showed widespread generalized pustules accompanied by high fever and elevation of circulating CRP to 30 mg/dl, which were triggered by infection, and he was hospitalized. A skin biopsy from a pustular eruption on the trunk revealed a spongiform pustule of Kogoj in the epidermis (Figure 1c), which is consistent with GPP. He was diagnosed as GPP unassociated with psoriasis vulgaris (PV) or palmoplantar pustulosis (PPP). There was no apparent family history of skin disorders, although his parents are first cousins (Figure 1d).

The ethics committee of Nagoya University approved studies described below. The study was conducted according to the Declaration of Helsinki Principles. The participants gave written informed consent. The coding region of *IL36RN* (Gene bank accession No. 26525) was amplified from genomic DNA by PCR, as described previously[1]. Direct sequencing of the patient's PCR products revealed that the patient was homozygous for the previously unreported nonsense mutation of p.Arg10X (c.28C>T) in *IL36RN* (Figure 2a). C at nucleotide position 28 is 2 bases upstream from the C' end of exon 2 (the exon 2-intron 2 boundary) of *IL36RN*. *In silico* analysis by splicing donor score algorithm[8] was conducted to predict whether this mutation would lead to aberrant or normal splicing, and the results suggest that this mutation results in normal splicing (data not shown).

Immunohistochemistry with rabbit polyclonal anti-IL1F5 antibody (R&D Systems Inc. Minneapolis, MN) showed almost no expression of IL36RN in the patient's epidermal lesion but strong IL36RN expression in a positive control of psoriatic epidermis (Figure 2b,c), as reported previously[9]. Thus, it was apparent that the IL36RN protein was almost absent in the patient.

Very recently, *IL36RN* mutations were reported as causative genetic defects in GPP cases in Tunisian and European populations[1, 2]. In these reports, only three missense mutation were identified: *IL36RN,* i.e., IL36RN pLeu27Pro in the Tunisian population[1], and p.Arg48Trp and p.Ser113Leu in the European population[2]. pLeu27Pro and p.Ser113Leu were thought to be very prevalent mutations in the respective (Tunisian and European) populations.

We report for the first time a GPP patient with an *IL36RN* mutation in an Asian population, and we note that the mutation differs from those prevalent in the Tunisian and European populations. In addition, the present mutation is the first documented nonsense mutation of *IL36RN.* It is nearly a null mutation of IL36RN, and its abolition or extreme reduction of the protein expression of IL36RN was confirmed in the patient's skin. Thus, the present case bolsters the argument that IL36RN functional deficiency really contributes to GPP.

It is interesting that the disease onset of the present case was the rather late age of 34, although the present case was homozygous for *IL36RN* loss-of-function mutation and had no apparent IL36RN protein. In previous reports, most GPP cases with *IL36RN* mutations have been children, though they included three young adults (disease onset in the twenties). The only exceptional case in previous reports was a patient whose age of onset was 51[2]. The present case suggests that even when onset is not until middle age, we cannot exclude the possibility of underlying *IL36RN* mutations as causative genetic defects.

In addition, it is noteworthy that no GPP cases with *IL36RN* mutations, including the present case, have been associated with PV or PPP[1, 2], and the absence of PV and PPP is a clue in identifying GPP patients with *IL36RN* mutations.

We believe it is very important to discriminate familial GPP cases with *IL36RN* mutations from the other GPP cases, not only for genetic counseling but also because we expect familial GPP will be treatable with customized therapy that targets IL-36 signaling in the near future.

References

1. Marrakchi S, Guigue P, Renshaw BR, et al. (2011) Interleukin-36-receptor antagonist deficiency and generalized pustular psoriasis. N Engl J Med 365:620-8
2. Onoufriadis A, Simpson MA, Pink AE, et al. (2011) Mutations in IL36RN/IL1F5 are associated with the severe episodic inflammatory skin disease known as generalized pustular psoriasis. Am J Hum Genet 89:432-7
3. Mulero JJ, Pace AM, Nelken ST, et al. (1999) IL1HY1: A novel interleukin-1 receptor antagonist gene. Biochem Biophys Res Commun. 263:702-6.
4. Smith DE, Renshaw BR, Ketchem RR, et al. (2000) Four new members expand the interleukin-1 superfamily. J Biol Chem 275:1169-1175
5. Dinarello C, Arend W, Sims J, et al. (2010) IL-1 family nomenclature. Nat Immunol 11:973.
6. Debets R, Timans JC, Homey B, et al. (2001) Two novel IL-1 family members, IL-1 delta and IL-1 epsilon, function as an antagonist and agonist of NF-kappa B activation through the orphan IL-1 receptor-related protein 2. J Immunol 167:1440-6
7. Towne JE, Garka KE, Renshaw BR, et al. (2004) Interleukin (IL)-1F6, IL-1F8, and IL-1F9 signal through IL-1Rrp2 and IL-1RAcP to activate the pathway leading to NF-kappaB and MAPKs. J Biol Chem 279:13677-88
8. Sahashi K, Masuda A, Matsuura T, et al. (2007) In vitro and in silico

analysis reveals an efficient algorithm to predict the splicing consequences of mutations at the 5' splice sites. Nucleic Acids Res 35:5995-6003

9. Blumberg H, Dinh H, Trueblood ES, et al. (2007) Opposing activities of two novel members of the IL-1 ligand family regulate skin inflammation. J Exp Med 204:2603-14

Figure Legends

Figure 1. Skin manifestation, histopathology of the skin lesion and pedigree of the patient

Pustular erythema on internal left knee of the patient (a, b). Spongiosis of Kogoj and acanthosis are observed in the epidermis of the pustular erythema lesion in the trunk upon the patient's admission to hospital (c). Bar: 100 μm. Pedigree of the patient (d).

Figure 2. Sequence data of *IL36RN* and expression of IL36RN on the lesion of the GPP

Sequence data of *IL36RN* in the patient and control (a). Arrow shows heterozygous mutation of c. 28C>T (p.Arg10Ter). C at nucleotide position 28 is 2 bases upstream from the C' end of exon 2 (the exon 2-intron 2 boundary) of *IL36RN*. Immunohistochemistry of GPP lesion by anti-IL1F5 (IL36RN) (b). Staining was almost negative. Immunohistochemistry of skin lesion of a patient with psoriasis vulgaris by anti-IL1F5 (IL36RN) (c). Staining was strong in keratinocytes in the upper layers. Bar: 100 μm.

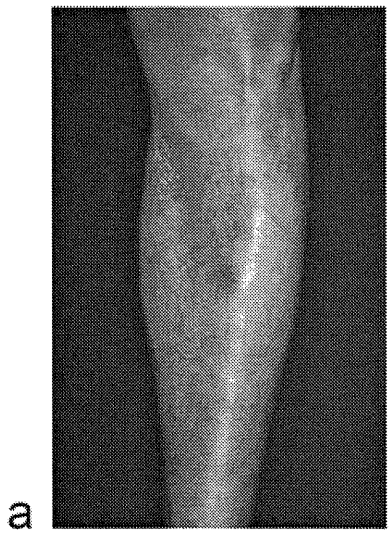

a

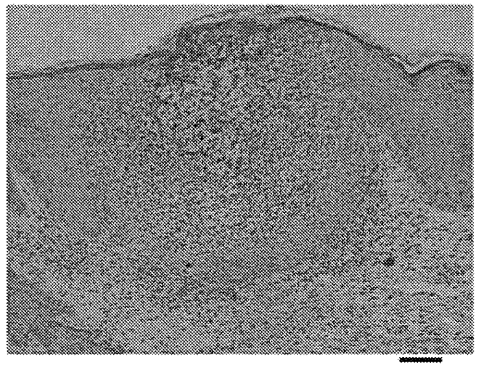

c

b

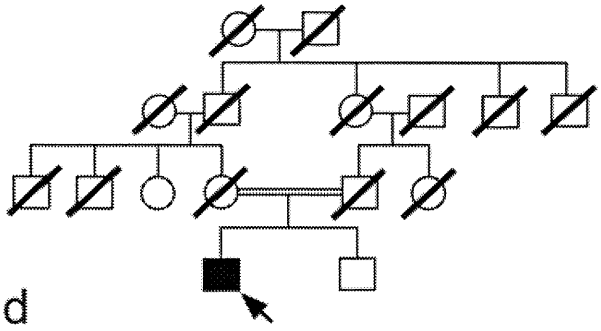

d

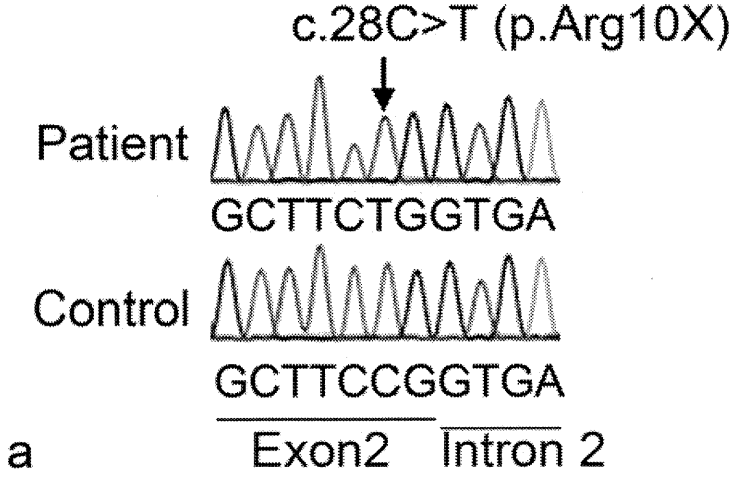
c.28C>T (p.Arg10X)
Patient
GCTTCTGGTGA
Control
GCTTCCGGTGA
Exon2
Intron 2

a

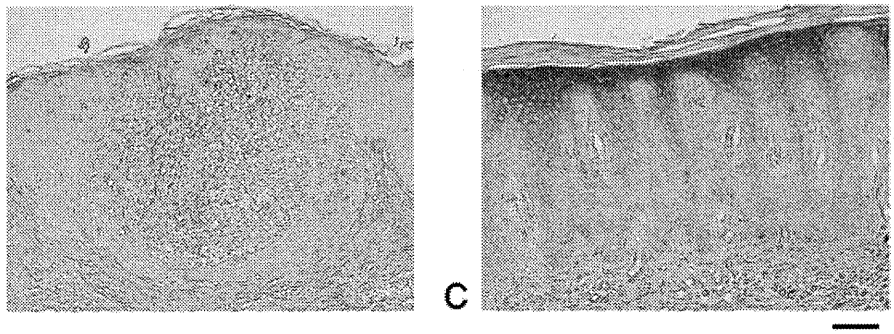

b c

SHORT REPORT

Prevalent founder mutation c.736T>A of *LIPH* in autosomal recessive woolly hair of Japanese leads to variable severity of hypotrichosis in adulthood

K. Tanahashi,[†] K. Sugiura,[†] T. Takeichi,[†,‡] H. Takama,[§] S. Shinkuma,[¶] H. Shimizu,[¶] M. Akiyama[†,*]

[†]Department of Dermatology, Nagoya University Graduate School of Medicine, 65 Tsurumai-cho, Showa-ku, Nagoya, Japan
[‡]Department of Dermatology, Inazawa City Hospital, Inazawa, Japan
[§]Takama Dermatology Clinic, Kasugai, Japan
[¶]Department of Dermatology, Hokkaido University Graduate School of Medicine, Sapporo, Japan
*Correspondence: M. Akiyama. E-mail: makiyama@med.nagoya-u.ac.jp

Abstract

Background Mutations in *LIPH* are a cause of autosomal recessive woolly hair (ARWH). Homozygous c.736T>A (p.Cys246Ser), and compound heterozygous c.736T>A and c.742C>A (p.His248Asn) have been reported in 5 and 7 Japanese children with ARWH respectively. The severity of hypotrichosis is known to be able to change in the clinical course, and the mutation patterns of *LIPH* do not always correlate with the severity of hypotrichosis in ARWH caused by other mutation sites of *LIPH*. However, all 12 Japanese children previously reported to have ARWH have shown similar severity of hypotrichosis.

Objective In this study, we investigated the clinical features and molecular basis of ARWH in patients including three adults (three adults and two children) from five non-related Japanese families.

Methods Five families of Japanese origin that presented with woolly hair were studied. The phenotype was confirmed by clinical examination. Direct automated DNA sequencing of the *LIPH* gene was performed to identify the mutations in our probands.

Results All patients had had woolly hair since birth. Homozygous c.736T>A mutations were found in four patients, including three adult cases, and compound heterozygous c.736T>A and c.742C>A mutations were found in one child patient. The two adults and two children had only sparse scalp hair, although one adult woman had mild hypotrichosis with long hairs.

Conclusion Some patients with homozygous c.736T>A can have a mild hypotrichosis phenotype with long hairs in adulthood.

Received: 1 February 2012; Accepted: 27 February 2012

Conflicts of interest

None to declare.

Funding sources

This study was supported in part by a Grant-in-Aid for Scientific Research, (A) 23249058 (M.A.) from the Ministry of Education, Culture, Sports, Science and Technology of Japan.

Introduction

Autosomal recessive woolly hair/hypotrichosis (ARWH: OMIM #278150/604379/611452) is a rare hereditary hair disease characterized by tightly curled hair at birth. It can lead to sparse hair later in life. The disease was shown to be caused by mutations in either the *LIPH* or the *LPAR6* gene.[1,2] The *LIPH* gene encodes a membrane-associated phosphatidic acid-preferring phospholipase $A_1\alpha$ (PA-PLA$_1\alpha$), which produces lysophosphatidic acid (LPA) from phosphatidic acid.[3] LPA is an extracellular mediator, which possesses many biological functions. The *LPAR6* gene encodes the G protein-coupled receptor LPA receptor 6 (LPAR6).[2] Both PA-PLA$_1\alpha$ and LPAR6 are abundantly expressed in human hair follicles, where their expression overlaps in the inner root sheath.[1,2] Thus, it has been postulated that PA-PLA$_1\alpha$ and LPAR6 are components of a common signalling pathway, which plays a crucial role in hair growth in humans.[2,4]

In Japanese, only two patterns of mutations have been reported: homozygous c.736T>A, and compound heterozygous c.736T>A

and c.742C>A of *LIPH*, in 12 children from 4 and 6 ARWH families respectively.[5–8] The *LIPH* mutations c.736T>A (p.Cys246Ser) and c.742C>A (p.His248Asn) were proven to be dysfunctional by *in vitro* studies.[6] Both missense mutations are considered extremely prevalent founder mutations for ARWH in the Japanese population.[6] The frequencies of the c.736T>A and c.742C>A alleles in healthy Japanese control individuals are 1.5% (3/200) and 0.5% (1/200) respectively, which implies the existence of many carriers for each mutation in the Japanese population.[6] Thus, it can be estimated that there are approximately 10 000 Japanese patients with ARWH carrying the *LIPH* mutations.

The mutation patterns of *LIPH* do not always correlate with the severity of hypotrichosis in ARWH. For example, affected individuals with homozygous mutation c.659–660delTA of *LIPH* showed significant differences in the severity of the hypotrichosis.[9] However, in the previous reports, all patients carrying homozygous mutations c.682delT or c.322T>C of *LIPH* have mild hypotrichosis,[9] and all patients harbouring homozygous mutations Ex4 deletion or c.346–350del of *LIPH* have severe hypotrichosis.[1,10] Therefore, some mutations of *LIPH* are thought to have genotype–phenotype correlation on severity of hypotrichosis in ARWH. As for c.736T>A, the prevalent *LIPH* mutation in the Japanese population, five Japanese children were reported to be homozygous for this mutation and all the children showed severe hypotrichosis, as we mentioned above.[5,6,8] Thus, all the patients homozyogous for c.736T>A were thought to have severe phenotype. However, the present study revealed that patients with this prevalent mutation possibly show mild hypotrichosis at least in the adulthood.

Materials and methods

Subjects

Five unrelated non-consanguineous Japanese families A, B, C, D and E (Fig. 1) with ARWH were seen in our hospital or referred to us in the previous 6 months. Family A was from Tokyo. Families B, C, D, and E were from Aichi Prefecture, in central Japan. The patients' ages and sexes are summarized in Table 1. The medical ethics committee of Nagoya University approved all the described studies. The study was conducted according to the Declaration of Helsinki Principles. The patients and families gave written informed consent.

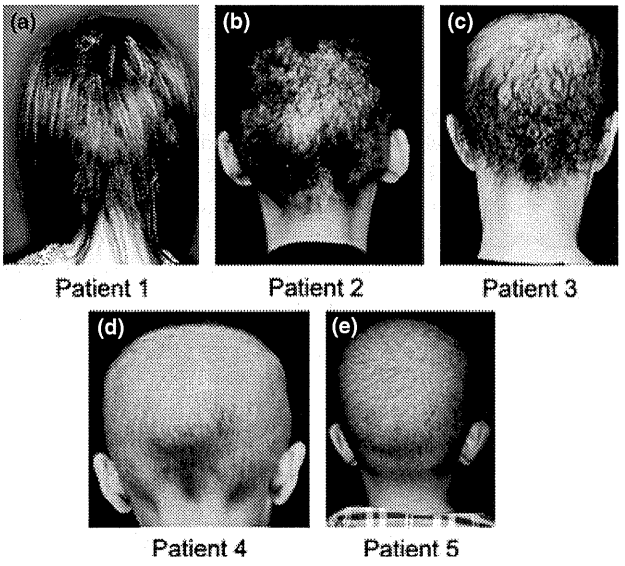

Figure 1 Clinical features of five Japanese families with ARWH. (a) Patient 1. (b) Patient 2. (c) Patient 3. (d) Patient 4. (e) Patient 5. All the affected individuals have features of ARWH, which is characterized by woolly hair on the scalp. In Patient 1, the hypotrichosis is notably mild and the hair is longer than in Patients 2 to 5. Scalp hairs of Patient 1 were treated with straight permanent wave.

Mutation detection

LIPH mutation search was performed as previously reported.[6] Briefly, genomic DNA (gDNA) isolated from peripheral blood was subjected to polymerase chain reaction (PCR) amplification, followed by direct automated sequencing using an ABI PRISM 3100 Genetic Analyzer (Advanced Biotechnologies, Columbia, MD, USA). The entire coding regions of *LIPH* including the exon/intron boundaries were sequenced using gDNA samples from patients and their family members.

Results

Clinical findings

All 5 affected individuals in the five unrelated Japanese families showed features of ARWH (Fig. 1). Eyebrows and eyelashes were slightly sparse to absent, although nails, teeth, sweating and

Table 1 Mutations in the *LIPH* gene in five families

Patient	Age	Sex	Family	*LIPH* mutation	Father	Mother	Sibling
1	25	F	A	c.736 T>A, homo	N.A.	c.736 T>A, hetero	
2	27	F	B	c.736 T>A, homo	N.A.	N.A.	
3	35	F	C	c.736 T>A, homo	N.A.	N.A.	
4	3	M	D	c.736 T>A, homo	c.736 T>A, hetero	c.736 T>A, hetero	c.736 T>A, hetero
5	4	M	E	c.736 T>A, c.742C>A, compound hetero	c.736 T>A, hetero	c.742 C>A, hetero	

N.A., not analysed.

hearing were normal in all the affected individuals. The hypotrichosis of one adult patient, Patient 1, was relatively less severe. Patient 1 had woolly hair and hypotrichosis at birth. According to the Patient 1, the hypotrichosis improved after treatment by herself with commercially available 1% minoxidil solution. She did not remember how long it took to improve the hypotrichosis. At the first visit to our hospitals, the scalp hairs were treated with straight permanent wave. Her hair was long enough without any cosmetic problem. She showed a much milder phenotype of the scalp hair than the other two adult patients, Patients 2 and 3. The two child patients had woolly hair with severe hypotrichosis. The heterozygous carriers of the *LIPH* mutations had normal hair.

Mutation detection

Direct sequencing analysis of exons and intron–exon boundaries of *LIPH* revealed that affected members of families A, B, C and D were homozygous for c.736T>A (p.Cys246Ser) (Table 1). The affected individual in Family E was compound heterozygous for the two missense mutations c.736T>A (p.Cys246Ser) and c.742C>A (p.His248Asn). All the patients' parents whose DNA was available for mutation search were heterozygous carriers of one of the two mutations (Table 1).

Discussion

In this study, we analysed five cases including three adults from five unrelated families with ARWH. All five cases had one or two of the two prevalent *LIPH* mutations in the Japanese population.[5–8] One 25-year-old woman had long hair with mild hypotrichosis, features that were extremely different from other adult cases.

ARWH caused by homozygous c.736T>A mutations, and compound heterozygous c.736T>A and c.742C>A mutations of *LIPH* are specific and common in the Japanese population. However, affected individuals who were previously reported have been under 10 years of age, and all the affected individuals have had sparse, curled hair that grew slowly from birth and then stopped growing after reaching a few inches. There have been no significant differences in clinical features between families and patients so far.[5–8] As ARWH patients with these mutations are estimated to be rather prevalent in Japan, it is important to know the clinical course of hypotrichosis of ARWH caused by these mutations. Patient 1 is a distinct example of an ARWH patient with hypotrichosis in childhood whose hypotrichosis phenotype improved in adulthood.

Patient 1 was administrated commercially available 1% minoxidil solution by herself before the first visit to our hospital. It was not certain whether the minoxidil solution really worked on the hypotrichosis of this case. Future large clinical studies might reveal whether the solution actually improves sparse scalp hairs of ARWH.

In conclusion, we presented the clinical features of three adult ARWH cases caused by the most prevalent mutation patterns of *LIPH* in Japan. This study suggests that the severity of hypotrichosis can decrease in adulthood.

Acknowledgements

We thank the patients and families for their generous cooperation. We also thank Dr. Hiroshi Kato for referral to us.

References

1 Kazantseva A, Goltsov A, Zinchenko R *et al.* Human hair growth deficiency is linked to a genetic defect in the phospholipase gene LIPH. *Science* 2006; **314**: 982–985.
2 Pasternack SM, von Kügelgen I, Aboud KA *et al.* G protein-coupled receptor P2Y5 and its ligand LPA are involved in maintenance of human hair growth. *Nat Genet* 2008; **40**: 329–334.
3 Sonoda H, Aoki J, Hiramatsu T *et al.* A novel phosphatidic acid-selective phospholipase A1 that produces lysophosphatidic acid. *J Biol Chem* 2002; **277**: 34254–34263.
4 Pasternack SM, von Kügelgen I, Müller M *et al. In vitro* analysis of LIPH mutations causing hypotrichosis simplex: evidence confirming the role of lipase H and lysophosphatidic acid in hair growth. *J Invest Dermatol* 2009; **129**: 2772–2776.
5 Shimomura Y, Ito M, Christiano AM. Mutations in the LIPH gene in three Japanese families with autosomal recessive woolly hair/hypotrichosis. *J Dermatol Sci* 2009; **56**: 205–207.
6 Shinkuma S, Akiyama M, Inoue A *et al.* Prevalent LIPH founder mutations lead to loss of P2Y5 activation ability of PA-PLA1alpha in autosomal recessive hypotrichosis. *Hum Mutat* 2010; **31**: 602–610.
7 Suga H, Tsunemi Y, Sugaya M *et al.* Hair shaft abnormalities in localized autosomal recessive hypotrichosis 2 and a review of other non-syndromic human alopecias. *Acta Derm Venereol* 2011; **91**: 486–488.
8 Yoshimasu T, Kanazawa N, Kambe N *et al.* Identification of 736T>A mutation of lipase H in Japanese siblings with autosomal recessive woolly hair. *J Dermatol* 2011; **38**: 900–904.
9 Shimomura Y, Wajid M, Petukhova L *et al.* Mutations in the lipase H gene underlie autosomal recessive woolly hair/hypotrichosis. *J Invest Dermatol* 2009; **129**: 622–628.
10 Ali G, Chishti MS, Raza SI *et al.* A mutation in the lipase H (LIPH) gene underlie autosomal recessive hypotrichosis. *Hum Genet* 2007; **121**: 319–325.

IJD 5548 B
Journal Name Manuscript No.
Dispatch: 4.4.12 Journal: IJD CE: GeethaPriya P.
Author Received: No. of pages: 2 PE: Prasanna
International Journal of Dermatology

Correspondence

Extraordinarily large, giant spider angioma in an alcoholic cirrhotic patient

Spider angioma/nevus, or nevus araneus, is a common cutaneous vascular anomaly, and is present in 10–15% of normal adults and children.[1] A spider angioma is typically a central, elevated, red punctum, from which blood vessels radiate 1–2 cm in diameter. We report here an extremely large spider angioma in a patient with liver cirrhosis.

A 68-year-old man with an 8-year history of alcoholic liver cirrhosis consulted our outpatient clinic complaining of a large reddish-purple soft tumor with radiating telangiectasia on the back. He had had the lesion for more than 1 year. The lesion had expanded and elevated gradually, and radiating telangiectasia appeared surrounding it. Subsequently, 10 or more small telangiectatic lesions appeared on his upper trunk and arms. He had been drinking about 50 g of alcohol per day until being diagnosed with liver cirrhosis. He had esophageal varices and was treated with endoscopic therapy. Physical examination revealed a reddish-purple, soft, dome-shaped node with a diameter of 2.3 × 1.3 cm, and telangiectasia radiating from the center to a diameter of 10 cm (Fig. 1). Multiple, typical spider angiomas of ordinary size (<2 cm in diameter) were scattered on his upper trunk and upper extremities. Laboratory studies showed liver dysfunction and decreased platelet count. A skin biopsy was taken from the central reddish-purple node. Histopathologically, dilated vessels of various sizes were observed to have proliferated in the superficial and mid dermis. Inflammatory cells, mainly lymphocytes and histiocytes, were infiltrated around the dilated vessels, and erythrocyte extravasation was also seen. Endothelial cells of the vessels were round and protruding into the lumen, although no atypism was observed (Fig. 2). From these clinical and histopathological features, the diagnosis of spider angioma was made. During the 6-month follow-up period, no remarkable changes were seen in either the liver cirrhosis or the spider angioma. The patient did not want any treatment for the angioma.

Spider angioma is seen in patients with pregnancy, thyrotoxicosis, oral contraceptive use and, most commonly, liver cirrhosis. Spider angiomas are known to be more common in patients with alcoholic cirrhosis than in those with viral or idiopathic cirrhosis. The pathogenesis of spider angioma is still unclear. Li *et al.*[2] reported an association between elevated plasma levels of vascular endothelial growth factor and spider angiomas. In patients with non-alcoholic cirrhosis, the plasma level of substance P is elevated, and this may play an important

LOW RESOLUTION COLOR FIG

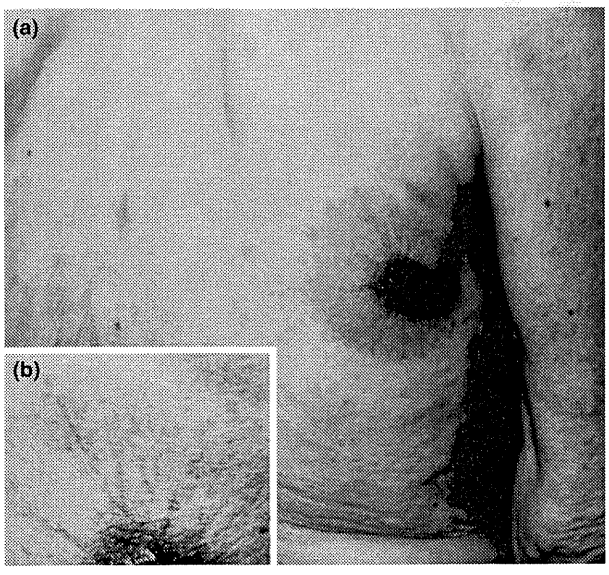

Figure 1 (a) A large reddish-purple soft tumor with radiating telangiectasia on the patient's back. (b) Close-up of the radiating telangiectasia. The clinical features of the present case are similar to those of a case reported previously[5]

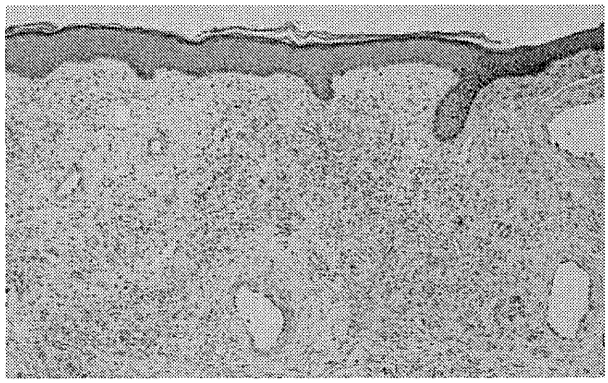

Figure 2 Photomicrograph of a skin biopsy specimen from the central node. Dilated vessels of various sizes are proliferated in the superficial and mid dermis. No atypism is observed in the endothelial cells. Low-density inflammatory cell infiltrate is observed around the dilated vessels (hematoxylin-eosin, original magnification ×100)

COLOR

role in the pathogenesis of spider angioma.[3] Estrogen also is suspected of playing a role.[4] Spider angiomas are usually <2 cm in diameter. Okada reported a giant spider angioma 6 cm in diameter.[5] As far as we know, the present spider angioma is the biggest ever reported. Generally, the central feeding vessel of spider angiomas can be destroyed with electrolysis or hyfrecation. Spider angiomas are also well treated by various types of lasers.[6,7] Giant spider angiomas can be treated by surgical excision.

The differential diagnosis for giant spider angioma includes several tumors of vascular origin, among them angiosarcoma, Kaposi's sarcoma and malignant hemangiopericytoma. Histopathological examination is often necessary to exclude these malignant tumors. Typical spider angiomas of ordinary size on the upper trunk and extremities were helpful in diagnosing the present case. Although giant spider angioma is rare, we have to keep it in mind in the differential diagnosis of large tumors of vascular origin, especially in patients with chronic liver diseases.

Hiroaki Hane, MD
Kenji Yokota, MD
Michihiro Kono, MD, PhD
Yoshinao Muro, MD, PhD
Masashi Akiyama, MD, PhD
Department of Dermatology, Nagoya University Graduate School of Medicine, Nagoya, Japan
E-mail: makiyama@med.nagoya-u.ac.jp

Funding: the authors have no funding sources for this work.

Conflicts of interest: the authors have no conflicts of interest to disclose.

doi: 10.1111/j.1365-4632.2012.05548.x

References

1 Requena L, Sangueza OP. Cutaneous vascular anomalies. Part I. Hamartomas, malformations, and dilation of preexisting vessels. *J Am Acad Dermatol* 1997; 37: 523–549; quiz 549–552.
2 Li CP, Lee FY, Hwang SJ, *et al.* Spider angiomas in patients with liver cirrhosis: role of vascular endothelial growth factor and basic fibroblast growth factor. *World J Gastroenterol* 2003; 9: 2832–2835.
3 Li CP, Lee FY, Hwang SJ, *et al.* Role of substance P in the pathogenesis of spider angiomas in patients with nonalcoholic liver cirrhosis. *Am J Gastroenterol* 1999; 94: 502–507.
4 Skafar DF, Xu R, Morales J, *et al.* Clinical review 91: female sex hormones and cardiovascular disease in women. *J Clin Endocrinol Metab* 1997; 82: 3913–3918.
5 Okada N. Solitary giant spider angioma with an overlying pyogenic granuloma. *J Am Acad Dermatol* 1987; 16: 1053–1054.
6 Dawn G, Gupta G. Comparison of potassium titanyl phosphate vascular laser and hyfrecator in the treatment of vascular spiders and cherry angiomas. *Clin Exp Dermatol* 2003; 28: 581–583.
7 Gupta G, Bilsland D. A prospective study of the impact of laser treatment on vascular lesions. *Br J Dermatol* 2000; 143: 356–359.

Author Query Form

Journal: IJD

Article: 5548

Dear Author,
During the copy-editing of your paper, the following queries arose. Please respond to these by marking up your proofs with the necessary changes/additions. Please write your answers on the query sheet if there is insufficient space on the page proofs. Please write clearly and follow the conventions shown on the attached corrections sheet. If returning the proof by fax do not write too close to the paper's edge. Please remember that illegible mark-ups may delay publication.

Many thanks for your assistance.

Query reference	Query	Remarks
1	AUTHOR: Figure 1 has been saved at a low resolution of 248 dpi. Please resupply at 300 dpi. Check required artwork specifications at http://authorservices.wiley.com/submit_illust.asp?site=1	

USING e-ANNOTATION TOOLS FOR ELECTRONIC PROOF CORRECTION

Required software to e-Annotate PDFs: Adobe Acrobat Professional or Adobe Reader (version 8.0 or above). (Note that this document uses screenshots from Adobe Reader X)
The latest version of Acrobat Reader can be downloaded for free at: http://get.adobe.com/reader/

Once you have Acrobat Reader open on your computer, click on the Comment tab at the right of the toolbar:

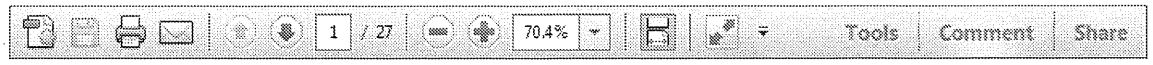

This will open up a panel down the right side of the document. The majority of tools you will use for annotating your proof will be in the Annotations section, pictured opposite. We've picked out some of these tools below:

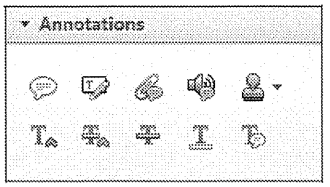

1. Replace (Ins) Tool – for replacing text.

Strikes a line through text and opens up a text box where replacement text can be entered.

How to use it

- Highlight a word or sentence.
- Click on the Replace (Ins) icon in the Annotations section.
- Type the replacement text into the blue box that appears.

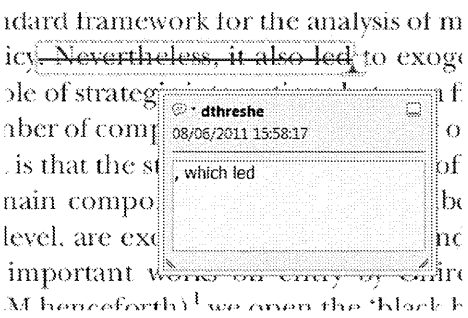

2. Strikethrough (Del) Tool – for deleting text.

Strikes a red line through text that is to be deleted.

How to use it

- Highlight a word or sentence.
- Click on the Strikethrough (Del) icon in the Annotations section.

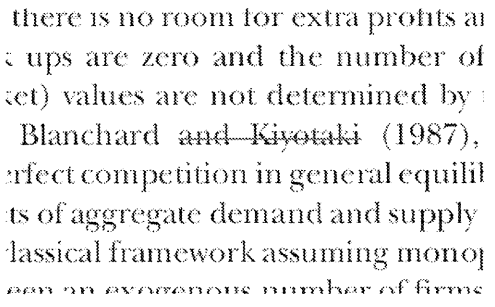

3. Add note to text Tool – for highlighting a section to be changed to bold or italic.

Highlights text in yellow and opens up a text box where comments can be entered.

How to use it

- Highlight the relevant section of text.
- Click on the Add note to text icon in the Annotations section.
- Type instruction on what should be changed regarding the text into the yellow box that appears.

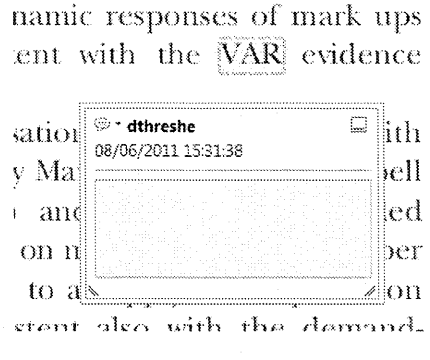

4. Add sticky note Tool – for making notes at specific points in the text.

Marks a point in the proof where a comment needs to be highlighted.

How to use it

- Click on the Add sticky note icon in the Annotations section.
- Click at the point in the proof where the comment should be inserted.
- Type the comment into the yellow box that appears.

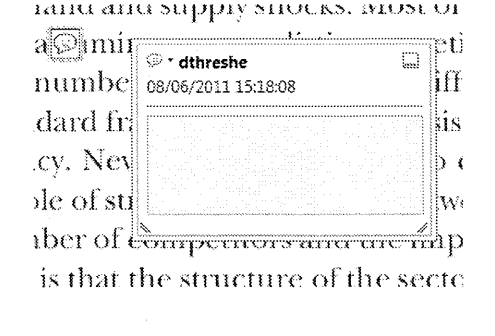

5. Attach File Tool – for inserting large amounts of text or replacement figures.

Inserts an icon linking to the attached file in the appropriate pace in the text.

How to use it

- Click on the Attach File icon in the Annotations section.
- Click on the proof to where you'd like the attached file to be linked.
- Select the file to be attached from your computer or network.
- Select the colour and type of icon that will appear in the proof. Click OK.

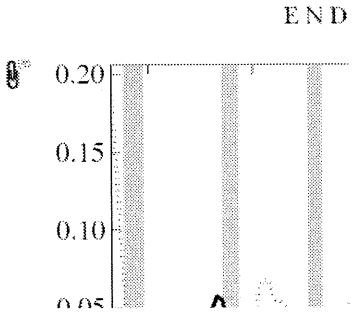

6. Add stamp Tool – for approving a proof if no corrections are required.

Inserts a selected stamp onto an appropriate place in the proof.

How to use it

- Click on the Add stamp icon in the Annotations section.
- Select the stamp you want to use. (The Approved stamp is usually available directly in the menu that appears).
- Click on the proof where you'd like the stamp to appear. (Where a proof is to be approved as it is, this would normally be on the first page).

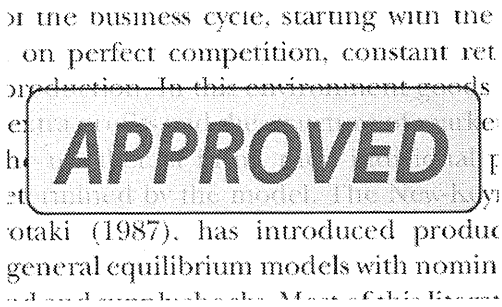

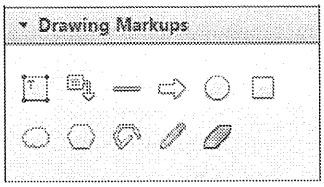

7. Drawing Markups Tools – for drawing shapes, lines and freeform annotations on proofs and commenting on these marks.

Allows shapes, lines and freeform annotations to be drawn on proofs and for comment to be made on these marks..

How to use it

- Click on one of the shapes in the Drawing Markups section.
- Click on the proof at the relevant point and draw the selected shape with the cursor.
- To add a comment to the drawn shape, move the cursor over the shape until an arrowhead appears.
- Double click on the shape and type any text in the red box that appears.

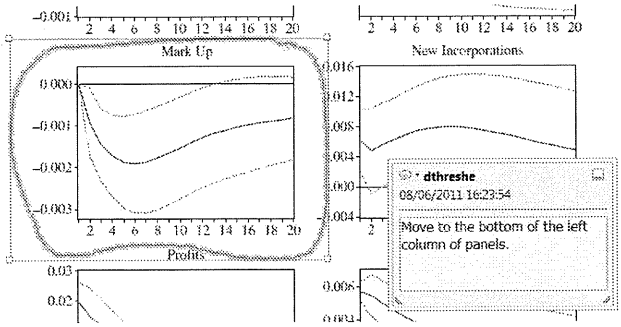

For further information on how to annotate proofs, click on the Help menu to reveal a list of further options:

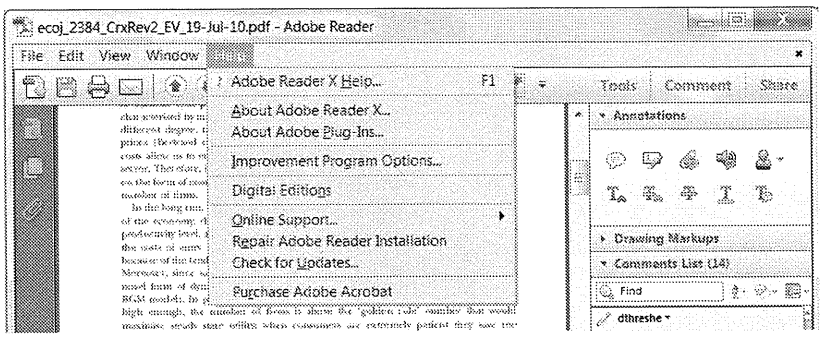

Rheumatology Advance Access published March 16, 2012
RHEUMATOLOGY

Original article

doi:10.1093/rheumatology/kes033

Development of an ELISA for detection of autoantibodies to nuclear matrix protein 2

Asuka Ishikawa[1], Yoshinao Muro[1], Kazumitsu Sugiura[1] and Masashi Akiyama[1]

Abstract

Objectives. Autoantibodies characterizing certain forms of inflammatory myopathy, which are myositis-specific autoantibodies, are useful in the diagnosis and prediction of prognosis in DM/PM. This study aimed to identify a subset of DM patients who have anti-nuclear matrix protein 2 (anti-NXP-2) antibodies by using biotinylated recombinant proteins, and to clarify the clinical features of DM patients with these antibodies.

Methods. Sera from 170 Japanese patients with CTDs including 106 with DM, 8 with PM, 21 with SLE, 20 with SSc, 15 with myositis overlap syndrome and 20 healthy controls were screened for anti-NXP-2 antibodies by our novel ELISAs. Positive sera were further examined by immunoprecipitation.

Results. Sera from 6 of the 170 patients with CTDs were confirmed to be positive for anti-NXP-2 antibodies. These six positives were from female patients, with five of the six sera being from adult DM patients and only one of the six being from 1 of the 12 JDM patients. All these patients had myositis. None of the anti-NXP-2-positive patients had interstitial lung disease, but one patient was complicated with ovarian cancer.

Conclusion. Our newly developed ELISA is applicable for the measurement of anti-NXP-2 antibodies. The results show that anti-NXP-2 antibodies, which have been characterized in JDM, exist in adult DM patients. Further studies using large populations are necessary to elucidate the characteristic clinical features and the prognosis of patients with anti-NXP-2 antibodies, especially for adult patients.

Key words: anti-MJ antibody, anti-NXP-2 antibody, dermatomyositis, ELISA, myositis-specific autoantibody.

Introduction

The idiopathic inflammatory myopathies (IIMs) are a group of acquired, systemic autoimmune diseases that include PM, DM and inclusion body myopathies [1, 2]. Several myositis-specific autoantibodies (MSAs) that are associated with certain clinical forms of IIMs have been identified, and they are useful tools for predicting the prognosis of IIMs. For example, anti-melanoma differentiation-associated protein 5 (MDA5)-antibody-positive patients demonstrate rapid progressive interstitial lung disease (ILD) and anti-transcriptional intermediary factor 1 (TIF1)-γ-antibody-positive patients are often complicated with cancer [3]. Recently anti-nuclear matrix protein 2 (anti-NXP-2, also called anti-MJ) antibodies that react to a 140-kDa polypeptide have been described in cohorts of JDM patients in the UK and Argentina [4].

Anti-NXP-2 antibodies were reported to be associated with calcinosis, although the antibodies were investigated only in cohorts of juvenile patients [4–6]. The prevalences of anti-NXP-2 antibodies in adult patients with CTDs have been unknown. We hypothesized that anti-NXP-2 antibodies could be detected not only in JDM patients, but also in adult DM cases, and that these antibodies could be a new serological marker for a certain disease subset of adult DM. To investigate the presence of anti-NXP-2 antibodies in sera from patients with various CTDs, this study used our newly developed ELISAs and immunoprecipitation (IPP) with biotinylated recombinant protein. We clarified the prevalence of the antibodies against NXP-2 in adult DM and examined clinical features associated with anti-NXP-2 antibodies.

[1]Department of Dermatology, Nagoya University Graduate School of Medicine, Showa-ku, Nagoya, Japan.

Submitted 9 October 2011; revised version accepted 25 January 2012.

Correspondence to: Yoshinao Muro, Division of Connective Tissue Disease and Autoimmunity, Department of Dermatology, Nagoya University Graduate School of Medicine, 65 Tsurumai-cho, Showa-ku, Nagoya 466-8550, Japan. E-mail: ymuro@med.nagoya-u.ac.jp

Materials and methods

Patients and sera

From the serum bank of the Department of Dermatology, Nagoya University Hospital, we used sera from 170 Japanese patients with CTDs. The CTD cohort consisted of 106 patients with DM [including 12 with JDM, 38 with clinically amyopathic DM (ADM) and 14 with cancer-associated DM], 8 with PM, 21 with SLE, 20 with SSc and 15 with myositis overlap syndrome (Table 1). The group of patients with myositis overlap syndrome consisted of seven patients with overlapping CTDs and eight with MCTD. Serum samples were collected at the time of diagnosis or before aggressive therapy. Twenty healthy Japanese individuals were also assessed as normal controls. All the DM patients, except those clinically ADM, and all the PM patients fulfilled Bohan and Peter's criteria [7, 8]. All the clinically ADM patients fulfilled Sontheimer's criteria [9]. The clinically ADM group included patients who had developed ILD within 6 months after disease onset. Patients were classified as having JDM if they were <16 years at the onset of DM according to the criteria of Bohan and Peter [10]. Patients were classified as cancer-associated DM if the internal malignancy was diagnosed within 3 years (before or after) of the DM diagnosis based on previous studies [11]. SLE was diagnosed by the ACR criteria for SLE [12]. SSc was diagnosed according to the SSc diagnostic criteria [13] established by the Ministry of Health, Labour and Welfare of Japan, which were modified from the ACR criteria [14]. MCTD was diagnosed according to the MCTD diagnostic criteria [15]. Patients were classified as having myositis in overlap with another CTD if they met published criteria for the CTD. The clinical records were retrospectively reviewed and the following information was recorded: demographic data including gender, age at onset, diagnosis, date of serum sampling and clinical features including the presence of cutaneous signs of DM (heliotrope rash or Gottron's papules), RP or calcinosis. Elevated creatine kinase (CK) was defined by elevation of CK above the normal range in clinical laboratory tests. Patients were diagnosed as having ILD, which was defined by fibrosis on chest radiographs or chest CT scans. Internal malignancy was investigated according to the results of whole-body CT, endoscopy, colonoscopy, gynaecological examination and breast cancer screening. The ages at the time of sera collection and gender ratios of each clinical group are summarized in Table 1. In the juvenile-onset patients with DM, two patients were originally seen at other hospitals far outside our area but then transferred to our hospital. Their intervals between disease onset and serum sampling were 26 and 28 years. All the patients and healthy individuals in the present study gave fully informed consent for participation, including provision of serum samples. This study was approved by the Ethics Committee of Nagoya University Graduate School of Medicine and conducted in accordance with the Declaration of Helsinki.

ELISAs

Specific binding of serum antibodies to recombinant NXP-2 was analysed using direct solid-phase ELISA. This method was based on our previous protocol, which quantitatively measured the antibodies against MDA-5 [16]. Instead of a conventional optical system for ELISA, this study used a microplate luminometer to increase the

TABLE 1 Patient's groups and anti-NXP-2 antibody frequencies

Clinical group	Age[a], range, years	Age[a], mean (S.D.), years	Gender, M:F	Total, *n*	α-NXP-2, *n* (%)
Total DM	3–84	51 (18)	33:73	106	6 (5.7)
Clinically ADM	3–84	48 (19)	9:29	38	0
Cancer-associated DM	48–80	66 (10)	6:8	14	1 (7.1)
Classical DM	16–80	49 (17)	18:36	54	5 (9.3)
Adult DM	19–84	55 (14)	26:68	94	5 (5.3)
Clinically ADM	23–84	54 (13)	5:27	32	0
Cancer-associated DM	48–80	66 (10)	6:8	14	1 (7.1)*
Classical DM	19–80	53 (15)	15:33	48	4 (8.3)*,**
JDM	3–32	18 (9)	7:5	12	1 (8.3)
Clinically ADM	3–32	16 (12)	4:2	6	0
Classical DM	16–27	20 (5)	3:3	6	1 (17)
Total other CTDs	18–75	45 (13)	6:58	64	0
PM	32–70	59 (13)	1:7	8	0
SLE	18–57	38 (11)	3:18	21	0
SSc	26–55	45 (8)	0:20	20	0
Overlap syndrome	24–75	49 (16)	2:13	15	0

[a]Age at the time of sera collection. In JDM, two patients were originally seen at other hospitals far outside our hospital. Their intervals between disease onset and serum sampling were 26 and 28 years. *$P < 0.05$ in classical adult DM and cancer-associated DM (5/62) *vs* other CTDs (0/64) by Fisher's exact test ($P = 0.0265$). **$P < 0.05$ in classical adult DM (4/48) *vs* other CTDs (0/64) by Fisher's exact test ($P = 0.0313$). M: male; F: female.

sensitivity, thereby reducing the required amount of biotinylated recombinant protein for the assays. The full-length NXP-2 cDNA clone was purchased from Kazusa DNA Research Institute (Chiba, Japan) and its DNA sequences were confirmed to be identical to GenBank accession number D50926. Biotinylated recombinant NXP-2 was produced from the cDNA, using the TnT T7 Quick Coupled Transcription/Translation System (Promega, Madison, WI, USA) according to our protocol [3]. Nunc Immobilizer Streptavidin Plates (Thermo Scientific Nunc, Roskilde, Denmark) to which streptavidin was covalently coupled via a spacer were pre-washed three times with PBS containing 0.05% Tween-20 (T-PBS) and were coated with biotinylated recombinant NXP-2 diluted with T-PBS (50 μl/well) and incubated for 1 h at room temperature with gentle agitation. After three washes with T-PBS, the wells were blocked with 200 μl of a blocking buffer of 0.5% BSA (Wako, Osaka, Japan) in T-PBS for 1 h. Uncoated wells were used to measure the background levels for each sample. Diluted sample sera with blocking buffer (50 μl/well) were incubated for 1 h at room temperature, followed by incubation with anti-human IgG antibody conjugated with HRP (Dako, Glostrup, Denmark) as a secondary antibody (50 μl/well) at 1:30 000 dilution after five washes. After incubation for 1 h at room temperature, the plates were washed five times and incubated with SuperSignal ELISA Femto Maximum Sensitivity Substrate (Thermo Scientific Pierce, Rockford, IL, USA) (50 μl/well) as the substrate according to the manufacturer's protocol. Then, the relative luminescence unit (RLU) was determined using the GloMax-Multi Detection System (Promega). Each serum sample was tested in duplicate, and the mean RLU subtracted background was used for data analysis. A standard curve was obtained from serial concentrations of a serum sample containing a high titre of the anti-NXP-2 antibody. The cut-off level was set at 17.0 U, based on 5 S.D. above the mean value obtained from 20 healthy control sera.

Detection of anti-NXP-2 antibodies using IPP

IPP was performed using transcription and translation (TnT) products as previously described [17–20], with minor modifications. Briefly, 10 μl of patient sera was mixed and incubated with 20 μl of a 50% slurry of Protein G Sepharose 4 Fast Flow (GE Healthcare, Buckinghamshire, UK) and 270 μl IPP buffer (PBS containing 1% Nonidet P-40) at 4°C for 1 h. Sepharose beads were mixed and incubated with 270 μl binding buffer (IPP buffer containing 0.5% BSA) and 10 μl of the TnT products, which was pre-cleared using the sepharose beads, at 4°C for 1 h. The beads were washed five times with IPP buffer, suspended in Laemmli sample buffer and the IgG-bound proteins retained by the sepharose beads were electrophoresed on 7.5% SDS-PAGE gel. The proteins were electrophoretically transferred onto Immobilon-P transfer membranes (Millipore Corporation, Billerica, MA, USA) and the biotinylated proteins were subsequently detected with Western Blue Substrate (Promega).

IIF

IIF was performed by standard methods [21] using HEp-2 cells (Fluoro HEPANA Test; MBL, Nagoya, Japan).

Statistical analysis

The frequency of antibodies between each CTD and control was analysed using Fisher's exact test. The associations between clinical features and antibodies in DM were analysed using Fisher's exact test or unpaired Student's *t*-test. SPSS version 17.0 for Windows (SPSS Japan, Tokyo, Japan) was used to perform the statistical analysis. $P < 0.05$ was considered statistically significant.

Results

Establishment of ELISA with biotinylated recombinant NXP-2

For the screening of anti-NXP-2 antibodies in large numbers of serum samples, we established an ELISA system that uses biotinylated recombinant NXP-2. In the present study, by using a luminometer, we succeeded in decreasing the required amount of TnT product for the assay from 10 μl/well in the previous system to 1 μl/well in our newly developed system, based on the results of serial dilution experiments (data not shown). We screened a total of 170 serum samples obtained from patients with various CTDs. Based on the cut-off level (17.0) at 5 S.D. above the mean value, six patients with DM and one patient with PM were classified into the anti-NXP-2-positive group (Fig. 1). When the cut-off was set at 3 S.D. above the mean value (9.7), one sample from a patient with SLE was just beneath the cut-off (9.2). Subsequently serum samples from these eight patients were used for IPP to confirm whether they were truly positive for the anti-NXP-2 antibodies.

Detection of anti-NXP-2 antibodies using IPP

After the initial screening by ELISA we investigated antibodies against NXP-2 in sera from 7 anti-NXP-2-positive patients, 1 equivocal patient and 24 anti-NXP-2-negative patients for their ability to immunoprecipitate biotinylated recombinant NXP-2. Six of the seven anti-NXP-2-positive sera in ELISA showed a distinct protein band with a molecular weight of 140 kDa in IPP assays (Fig. 2, lanes 1–6). All were from patients with DM, whereas the serum from the one patient with PM did not react to the recombinant (Fig. 2, lane 7). The serum from an SLE patient with an equivocal level of anti-NXP-2 antibodies in ELISA was negative in IPP (Fig. 2, lane 8). Furthermore, anti-NXP-2 antibodies were not detected in normal control sera as well as 24 anti-NXP-2-negative sera in ELISA by IPP assays (representative negative sera, Fig. 2, lane 9).

Clinical and serological features of DM patients with anti-NXP-2 antibodies

Of the 106 DM sera, 6 (5.7%) had anti-NXP-2 antibodies (Table 1). In contrast, anti-NXP-2 antibodies were not detected in any serum from patients with other CTDs.

FIG. 1 ELISA using biotinylated recombinant NXP-2 protein. Measurement of anti-NXP-2 antibodies in 170 serum samples from patients with various CTDs or 20 healthy control subjects. We used the 1 μl/well of TnT mixture and the diluted patient serum samples at 1:1000 for measuring all samples (closed circles). The antibody units were calculated from the RLU using a standard curve obtained from serial concentrations of a serum sample containing a high titre of the anti-NXP-2 antibody. Broken line indicates the cut-off value (17.0 U). Six samples from patients with DM, one sample from a patient with PM (grey circle, just around the cut-off value) and one sample from a patient with SLE (open circle, under the mean values of 20 healthy controls + 3 S.D.) were introduced to IPP assays with biotinylated recombinant proteins (see Fig. 2).

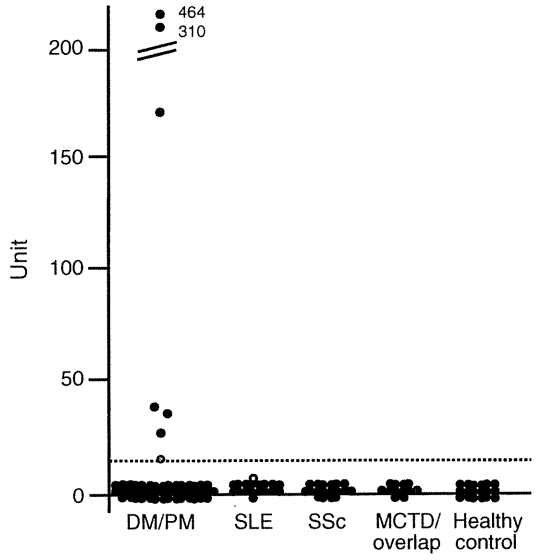

Anti-NXP-2 antibodies were found at a higher frequency in DM patients than in patients with other CTDs (6/106 *vs* 0/64, $P = 0.0844$). Concerning JDM, only 1 (8.3%) of the 12 JDM patients had serum that reacted with NXP-2. The patient with anti-NXP-2 antibodies had no findings associated with calcinosis. As for adult DM, sera from 5 (5.3%) of 94 patients were positive. In adult cancer-associated DM, serum from 1 (7.1%) of 14 patients was positive for anti-NXP-2 antibodies. This patient had ovarian cancer that resulted in a fatal outcome. Adult patients with classical DM had anti-NXP-2 antibodies with a significantly higher frequency than patients with other CTDs (4/48 *vs* 0/64, $P = 0.0313$). Even if adult patients with cancer-associated DM were added to the classical adult DM group, a significant difference would still remain between adult patients with DM and patients with other CTDs (5/62 *vs* 0/64, $P = 0.0265$). According to these results, anti-NXP-2 antibodies were detected not only in JDM, but also in cancer-associated adult DM and classical adult DM. No patients with any other CTD, clinically ADM or healthy individuals had anti-NXP-2 antibodies.

FIG. 2 IPP of biotinylated recombinant NXP-2 with patient's sera. The input lane contains half the dose (5 μl) of biotinylated recombinant NXP-2 protein that was used for the IPP assay. The band in this lane that migrated at around 140 kDa corresponds to NXP-2. Lanes 1–6 contain the NXP-2 immunoprecipitated by the sera of patients that were anti-NXP-2-positive in ELISA. Lane 7 is the serum that was just above the cut-off level in ELISA. Lane 8 is the equivocal serum in ELISA. Lane 9 is serum from a healthy control. We arranged the samples from lanes 1–9 according to the levels of ELISA units. The asterisk denotes biotinylated NXP-2.

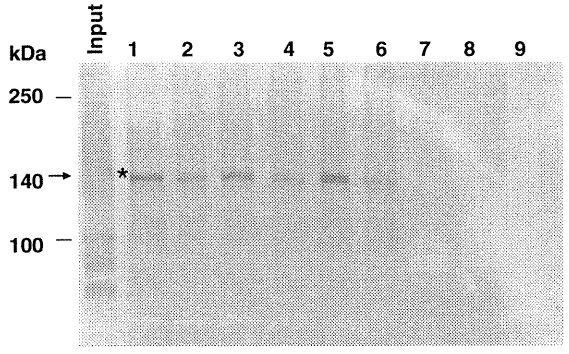

Table 2 compares the clinical features between anti-NXP-2-positive patients and anti-NXP-2-negative patients. There was little significant difference in gender, age at onset, diagnosis or prevalence of DM-specific skin symptoms (heliotrope rash and Gottron's papules or sign) and RP. All six of the anti-NXP-2-positive patients had myopathy, but none of them were complicated with ILD. The frequency of calcinosis was relatively higher in the positive group, although the difference was not significant.

Table 3 summarizes the serological information of the six patients with anti-NXP-2 antibodies in the present study. IIF revealed diverse nuclear staining patterns with various titres in all the anti-NXP-2-positive sera. The IIF titres did not correspond well to the ELISA units.

Discussion

There is increasing evidence that MSAs are associated with clinical subsets of DM/PM. Several MSAs have shown positive polypeptide bands ~140–160 kDa on SDS-PAGE by the traditional assay of IPP with cell extracts, including anti-NXP-2, anti-Mi-2, anti-MDA-5, anti-TIF1-γ and anti-OJ antibodies. It is difficult to differentiate these antibodies by molecular weight. We used biotinylated recombinant proteins and successfully detected anti-MDA-5 and anti-TIF1-γ antibodies in our IPP study [3]. However, there are technical limits to handling large numbers of serum samples efficiently with IPP. Thus we needed to establish an ELISA system. In our previous study, taking advantage of the high affinity between biotin